

# The X-ray emission properties and the dichotomy in the central stellar cusp shapes of early-type galaxies

S. Pellegrini\*

*Astronomy Department, University of Bologna, via Ranzani 1, 40127 Bologna, Italy*

Received ...; accepted ...

## ABSTRACT

*Hubble Space Telescope* revealed a dichotomy in the central surface brightness profiles of early-type galaxies, that subsequently have been grouped into two families: core, boxy, anisotropic systems and cuspy (“power law”), disk, rotating ones. Here we investigate whether a dichotomy is present also in the X-ray properties of the two families. We consider both their total soft emission ( $L_{\text{SX,tot}}$ ), that is a measure of the galactic hot gas content, and their nuclear hard emission ( $L_{\text{HX,nuc}}$ ), mostly coming from *Chandra* observations, that is a measure of the nuclear activity. At any optical luminosity, the highest  $L_{\text{SX,tot}}$  values are reached by core galaxies; this is explained with their being central dominant galaxies of groups, subclusters or clusters, in many of the  $\log L_{\text{SX,tot}} \text{ (erg s}^{-1}\text{)} \gtrsim 41.5$  cases. The highest  $L_{\text{HX,nuc}}$  values, similar to those of classical AGNs, in this sample are hosted only by core or intermediate galaxies; at low luminosity AGN levels,  $L_{\text{HX,nuc}}$  is independent of the central stellar profile shape. The presence of optical nuclei (also found by *HST*) is unrelated with the level of  $L_{\text{HX,nuc}}$ , even though the highest  $L_{\text{HX,nuc}}$  are all associated with optical nuclei. The implications of these findings for the galaxy evolution and the accretion modalities at the present epoch are discussed.

**Key words:** galaxies: elliptical and lenticular, CD – galaxies: evolution – galaxies: fundamental parameters – galaxies: nuclei – X-rays: galaxies – X-rays: ISM

## 1 INTRODUCTION

*Hubble Space Telescope* observations of the central surface brightness profiles  $I(R)$  of nearby early-type galaxies revealed that the profile shape has a bimodal distribution: either  $I(R)$  breaks internally to shallower shapes  $I \propto R^{-\gamma}$ , with  $\gamma < 0.3$ , and the corresponding galaxies are said to have cuspy cores; or  $I(R)$  follows a steep featureless power law that lacks a core down to the resolution limit, with a slope  $\gamma > 0.5$  (Ferrarese et al. 1994, Lauer et al. 1995, Faber et al. 1997; see also Trujillo et al. 2004). The core profile is typical of the most luminous ( $L_B \gtrsim 2.5 \cdot 10^{10} L_{B\odot}$ ) galaxies, while the featureless power law profile is typical of the least luminous ones; at intermediate luminosities, core and power law galaxies coexist. More recently, Ravindranath et al. (2001) and Rest et al. (2001) have identified a few systems with intermediate cusp slopes ( $0.3 < \gamma < 0.5$ ) that are however relatively uncommon, and the overall bimodal distribution of the central profile shapes appears to be robust (Lauer et al. 2005).

The division into two distinct classes of central struc-

ture was emphasized further when the dynamical and morphological properties of the galaxies were also considered: core galaxies are slow rotators and have boxy or elliptical isophotes, while power law galaxies are rapid rotators with disk isophotes (Kormendy & Bender 1996, Faber et al. 1997). These differences hold even when comparing power law and core galaxies of the same luminosity. All this suggested that the origin of the inner cusps is closely linked to the formation and subsequent evolution of the galaxies; for example, the merging of galaxies of comparable mass was conjectured to be responsible for creating cores and boxy isophotes, while the steep density cusps were linked to dissipation and therefore, possibly, to gas rich mergers or minor mergers with less massive companions (Faber et al. 1997; Naab & Burkert 2003).

Another major *HST* result is the widely accepted notion that massive black holes (MBHs) are ubiquitous in the centers of spheroids (e.g., Richstone et al. 1998) and that relationships exist between the MBH masses and the luminosity, central stellar velocity dispersion and central light concentration of their hosts (e.g., Tremaine et al. 2002, Graham et al. 2001). Therefore, there seems to be also a deep relationship between MBHs and their associated galaxies. In

\* E-mail: silvia.pellegrini@unibo.it

this context, many efforts have recently been made to link the creation of cusps and cores to the effects of MBHs, as they should have substantial influence on the dynamics and evolution of the surrounding gas and stars (e.g., Cipollina & Bertin 1994, van der Marel 1999, Milosavljevic et al. 2002). A popular scenario currently figures out that during the merging of galaxies, each harboring a central MBH, dynamical friction causes the MBHs to form a binary; interactions between the binary and the surrounding stars (or gas) would harden the binary until its coalescence, with ejection of stars from the center and the production of a core.

In this paper we investigate whether a dichotomy is present also in the X-ray properties of core and power law galaxies. In fact both the origin of the inner cusps, closely linked to the evolution of galaxies, and the presence of a MBH are expected to have an influence on the X-ray properties. In particular, the information coming from this wavelength allows us to investigate the relationship of  $\gamma$  with the galactic hot gas content (that manifests itself in the soft X-ray band; e.g., Kim et al. 1992) and with the nuclear AGN-like properties, that dominate in the hard X-ray band (Loewenstein et al. 2001, Pellegrini 2005). In an earlier work, Pellegrini (1999) investigated whether power law and core galaxies differ systematically in their soft X-ray luminosities. By using the data available at that time, coming from WFPC1, it was found that core galaxies can have a largely varying hot gas content, from being devoid of hot gas to being gas rich; on the contrary, power law galaxies are all confined to a more modest hot gas content. This held even in the range of optical luminosities where the two families coexist, and therefore the soft X-ray emission was considered another property distinguishing the two families of core and power law galaxies. Since then, the inner stellar light profiles have been observed again with the improved resolution of WFPC2, and larger samples with more homogeneous measurements of  $\gamma$  have been produced (Rest et al. 2001, Ravindranath et al. 2001, Lauer et al. 2005). As a result of the improved central profiles' characterization, a number of galaxies have been reclassified.

Here the problem of the relationship between the global hot gas content and the inner stellar cusps is revisited by taking advantage of the new samples of galaxies with  $\gamma$  measured, as well as of larger samples with the soft X-ray emission measured (O'Sullivan et al. 2001a). In addition, we can now investigate for the first time whether there is a relation between the central structure of galaxies and the presence or absence of nuclear activity. In fact, accurate measurements of the nuclear X-ray emission have become available recently thanks to *Chandra* observations (e.g., Pellegrini 2005) and a deep exploitation of the archival *ROSAT* HRI observations (Roberts & Warwick 2000, Liu & Bregman 2005). Finally, in a substantial fraction of the photometrically investigated galaxies *HST* showed nuclei, i.e., compact light sources that rise above the inward extrapolated surface brightness cusp at small radii, as residuals of the  $I(R) \propto R^{-\gamma}$  law fits (Lauer et al. 1995, Ravindranath et al. 2001, Rest et al. 2001). The origin of these optical nuclei is still uncertain; their relationship with the nuclear activity is investigated here by using the nuclear hard X-ray emission.

## 2 THE SAMPLE

All early-type galaxies with “Nuker law” parametric fits of their inner brightness profiles observed with *HST* were collected. In this fit the data are modeled with a double power law with a break radius, and the value of the inner surface brightness slope (the  $\gamma$  parameter) gives the classification into core or power law galaxy (e.g., Faber et al. 1997). In a few cases the central profile can even be declining ( $\gamma < 0$ , Lauer et al. 2005); few galaxies have  $0.3 < \gamma < 0.5$  and are termed intermediate. There is no specific criterion that characterizes this sample of galaxies with central brightness parameters, in general it comprises relatively luminous nearby ellipticals and S0s. The original work by Faber et al. (1997) made use of WFPC1 observations; in more recent times, most of these galaxies were re-observed with WFPC2. Therefore, when a galaxy has been studied more than once, its  $\gamma$  is taken here following this priority: first the sample of 77 galaxies imaged with *HST*+WFPC2 of Lauer et al. (2005) is considered; next that of 67 galaxies observed with *HST*+WFPC2 and studied by Rest et al. (2001); next that of 61 galaxies by Faber et al. (1997); next that of 33 galaxies observed with *HST*+NICMOS by Ravindranath et al. (2001); finally, the *HST*+NICMOS sample by Quillen et al. (2000) and the WFPC1-based works of Crane et al. (1993) and Ferrarese et al. (1994).

For this total sample of galaxies with information on the inner shape of the optical profile, the literature has been searched for the global soft X-ray emission (hereafter  $L_{\text{SX,tot}}$ ) and the nuclear hard emission in the 2–10 keV band (hereafter  $L_{\text{HX,nuc}}$ ). Almost all galaxies have  $L_{\text{SX,tot}}$  listed in the large catalogue based on *ROSAT* PSPC observations, that were sensitive over 0.1–2.4 keV, of O'Sullivan et al. (2001a). This catalogue includes all the early type galaxies with a Virgo corrected recession velocity  $v \leq 9000$  km s<sup>-1</sup> and apparent magnitude  $B_T \leq 13.5$ , and gives their  $L_{\text{SX,tot}}$  derived by fitting the data with a MEKAL hot plasma model of temperature  $kT = 1$  keV and solar metal abundance. For 8 galaxies  $L_{\text{SX,tot}}$  comes from other studies (based on *ROSAT* data in 6 cases<sup>1</sup> and on *Einstein* data for NGC2841 and NGC4342, Fabbiano et al. 1992).

The nuclear hard luminosity  $L_{\text{HX,nuc}}$  derives instead from a variety of works. Care was taken to draw as many measurements as possible from *Chandra* pointings, that have the best angular resolution so far ( $\sim 0''.5$ ); this was the case for most of the nuclei (34). Next, *ROSAT* HRI pointings have been considered (with an angular resolution of  $\sim 5''$ ) and these gave  $L_{\text{HX,nuc}}$  for 17 galaxies; finally, *XMM*–Newton pointings gave  $L_{\text{HX,nuc}}$  for NGC5548 and NGC7213, and *ASCA*, with a much larger angular resolution ( $\sim 3'$ ), gave  $L_{\text{HX,nuc}}$  for 3 cases (NGC3065, NGC3607, NGC7743), where the nuclei are considered to dominate the emission. All nuclear luminosities have been converted to the 2–10 keV band by using the spectral parameters found by the authors who analyzed the X-ray data.

Table 1 lists the 116 galaxies with both  $\gamma$  and  $L_{\text{SX,tot}}$  measured. This sample is almost double as large as

<sup>1</sup> These are: NGC524 (Heldson et al. 2001), NGC4494 (O'Sullivan & Ponman 2004), NGC4594 (Fabbiano & Juda 1997), NGC4874 and NGC4881 (Dow & White 1995), IC4329 (Irwin & Sarazin 1998).

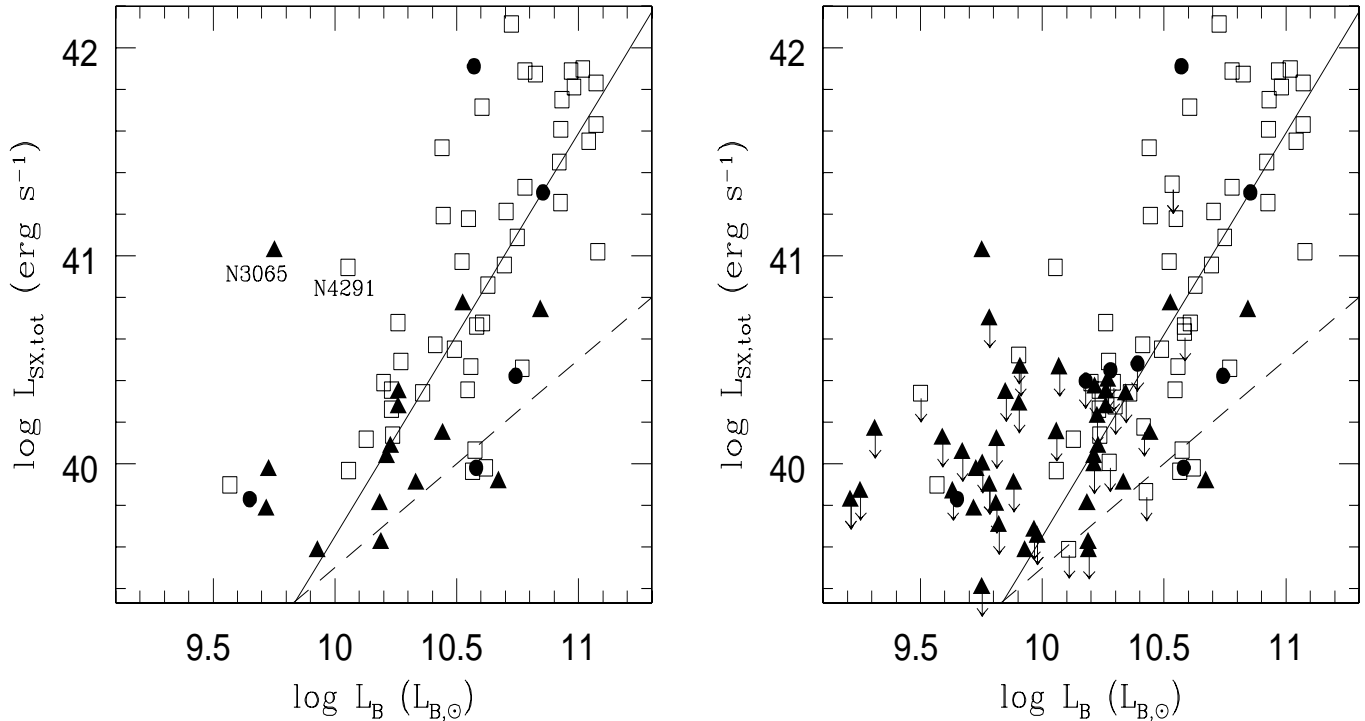


**Figure 1.** The total soft X-ray luminosity  $L_{\text{SX,tot}}$  versus the total B-band luminosity  $L_{\text{B}}$  for early-type galaxies with inner surface brightness profile measured by *HST* (detections only in the left panel, all data in the right panel, with upper limits on  $L_{\text{SX,tot}}$  shown with a downward arrow). Full triangles indicate power law galaxies, full circles intermediate ones and open squares core ones. The solid line is the best fit  $L_{\text{SX,tot}} - L_{\text{B}}$  relation for early-type galaxies and the dashed line is an estimate for the contribution to  $L_{\text{SX,tot}}$  from stellar sources (O’Sullivan et al. 2001a). Table 1 includes also the core galaxies NGC404 and 5 others with  $\log L_{\text{SX,tot}}$  ( $\text{erg s}^{-1}$ )  $> 42.2$  (all at  $\log L_{\text{B}} (L_{\text{B}\odot}) \geq 10.86$ ), and 5 power law galaxies with  $\log L_{\text{SX,tot}}$  ( $\text{erg s}^{-1}$ )  $< 39.4$  (all at  $\log L_{\text{B}} (L_{\text{B}\odot}) < 9.7$ ); these do not appear in the plot due to the boundary limits chosen to better show the region where both galaxy types coexist.

that considered by Pellegrini (1999), that included 59 objects. In addition, the present sample differs from the old one also because of some new features: it includes a few core galaxies at  $\log L_{\text{B}} (L_{\text{B}\odot}) < 10.2$  and the intermediate galaxies, a few power law galaxies of the old sample have been re-classified as core or intermediate galaxies, and a few X-ray upper limits in the old sample are now detections. Table 2 lists the 56 galaxies for which a search for the nuclear emission has been performed (5 of these are not in Table 1).

The Tables also list the blue luminosities  $L_{\text{B}}$  of the galaxies, taken from O’Sullivan et al. (2001a) or calculated from the  $B_T$  magnitudes of the LEDA catalogue, as done by O’Sullivan et al. (2001a). The distances used here are instead those homogeneously derived from the SBF method of Tonry et al. (2001). When this kind of distance is not available, the Lauer et al.’s or the O’Sullivan et al.’s distances or the distance used for the X-ray analysis (in this order) are adopted, after rescaling for the  $H_0 = 74 \text{ km s}^{-1} \text{ Mpc}^{-1}$  (as implied by Tonry et al. 2001). The  $L_{\text{SX,tot}}$ ,  $L_{\text{HX,nuc}}$  and  $L_{\text{B}}$  values in Table 1 and 2 have been rescaled for the distances adopted here.

### 3 RESULTS

#### 3.1 $L_{\text{SX,tot}}$ and inner light profile

In Fig. 1 the  $L_{\text{SX,tot}} - L_{\text{B}}$  relation for the galaxies in Table 1 is plotted, with different symbols for core, intermediate and power law systems. As found in general (Sect. 1), core galaxies are more frequent at higher  $L_{\text{B}}$ , while power law ones are more common at lower  $L_{\text{B}}$ .

Figure 1 shows that the most X-ray luminous galaxies are core and intermediate ones; also, for  $\log L_{\text{B}} (L_{\text{B}\odot}) > 10.4$  these cover the whole range of observed  $L_{\text{SX,tot}}$  values, that extends for roughly two orders of magnitude. Power law systems are instead confined below  $\log L_{\text{SX,tot}}$  ( $\text{erg s}^{-1}$ )  $\sim 41$ ; they tend to be less luminous than core ones at every  $L_{\text{B}}$ , with a marked difference at  $\log L_{\text{B}} (L_{\text{B}\odot}) > 10.4$ .

A statistical analysis has been performed to quantify how strong is this apparent dichotomy in the soft X-ray properties of core and power law galaxies. A series of Kolmogorov-Smirnov and Two Sample Tests (contained in the ASURV package, Feigelson & Nelson 1985) have been applied to establish first whether core and power law galaxies are consistent with being drawn from the same  $L_{\text{B}}$  distribution, and then whether they are also consistent with the same  $L_{\text{SX,tot}}$  distribution. Two intervals of  $L_{\text{B}}$  values have been considered: a larger one where the two

families overlap [ $10.0 < \log L_B (L_{B\odot}) < 10.7$ ], and the  $10.0 < \log L_B (L_{B\odot}) \leq 10.4$  region, where there is an equal number of core and power law galaxies (15 each). In the large  $L_B$  interval, the hypothesis of the same  $L_B$  distribution can be excluded at the  $\sim 2.4\sigma$  level only, while that of the same  $L_{SX,tot}$  distribution is excluded at the  $\sim 3.2\sigma$  level. In the small  $L_B$  interval, the two families are definitely consistent with having the same  $L_B$  distribution, while the hypothesis of the same  $L_{SX,tot}$  distribution can be excluded at the  $\sim 2.6\sigma$  level.

At  $\log L_B (L_{B\odot}) > 10.4$ , where the dichotomy in  $L_{SX,tot}$  is more evident, there are in Fig. 1 many more core systems than power law ones, and therefore the confinement of the latter to lower  $L_{SX,tot}$  could be coincidental. However, all the power law galaxies still lacking a measurement of  $L_{SX,tot}$  have  $\log L_B (L_{B\odot}) \leq 10.2$ . Consequently, Fig. 1 is already representative of the soft X-ray properties of the power law family presently known. Note also how there are just 4 intermediate galaxies at  $\log L_B (L_{B\odot}) > 10.4$ , yet these show a range of  $L_{SX,tot}$  fully comparable to that of core systems. Therefore, intermediate galaxies share the same soft X-ray properties of core ones.

Finally, note that the highest  $L_{SX,tot}$  value of power law galaxies (that of NGC3065, evidenced in Fig. 1) can be mostly ascribed to nuclear activity<sup>2</sup>. Therefore the soft X-ray emission due to hot gas is really confined below  $\sim 10^{41}$  erg s<sup>-1</sup> for all power law galaxies. On the other hand, the  $L_{SX,tot} > 10^{41}$  erg s<sup>-1</sup> values of most core and intermediate galaxies cannot be attributed totally or substantially to nuclear activity, given the generally low or very low emission level of the latter (Sect. 3.2, Table 2).

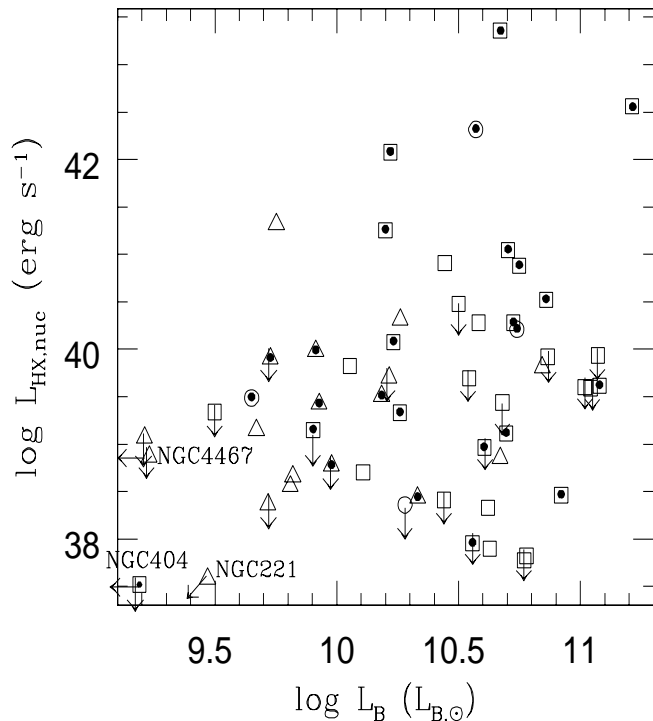
### 3.2 $L_{HX,nuc}$ and inner light profile

Figure 2 shows the relationship between the hard nuclear emission  $L_{HX,nuc}$  (from Table 2) and the galactic  $L_B$ , for core, intermediate and power law galaxies. This figure indicates that the galaxies with known  $L_{HX,nuc}$  cover the same large range of  $L_B$  values of Fig. 1. The relationship between  $L_{HX,nuc}$  and the inner optical profile shape  $\gamma$  is plotted in Fig. 3, which shows that:

1) core and intermediate galaxies span the whole range of  $L_{HX,nuc}$  values observed, from those typical of the faintest detected nuclei up to values typical of “classical” AGNs as Seyfert galaxies.

2) power law systems only host low luminosity AGNs, i.e., nuclei with  $L_{HX,nuc} \lesssim \text{few} \times 10^{41}$  erg s<sup>-1</sup> (e.g., Terashima et al. 2002). Their highest  $L_{HX,nuc}$  is that of NGC3065 (evidenced in Fig. 3); since it derives from ASCA data, it could have been somewhat overestimated, but a low luminosity AGN is certainly present in this galaxy, given that it hosts a LINER with broad Balmer lines (Eracleous & Halpern 2001) and its  $L_{HX,nuc}$  is 10 – 100 times higher than expected from

<sup>2</sup> The predicted *nuclear* luminosity over 0.1–2.4 keV, obtained by using the Iyomoto et al. (1998) spectral shape (Table 2), is  $\sim L_{SX,tot}$  derived by O’Sullivan et al. (2001a). On the contrary, the core galaxy NGC4291 close to NGC3065 (Fig. 1) has  $L_{SX,tot}$  mostly due to a hot ISM, since its nuclear emission accounts for  $\sim 0.15$  of  $L_{SX,tot}$  (for the spectral shape of the reference in Table 2).



**Figure 2.** The 2–10 keV nuclear luminosity  $L_{HX,nuc}$  versus the galactic  $L_B$  for early-type galaxies with inner surface brightness profile measured by *HST*. Power law galaxies are shown with triangles, intermediate ones with circles and core ones with squares. Upper limits on  $L_{HX,nuc}$  are shown with a downward arrow. The data used are those in Table 2. Galaxies with optical nuclei have a dot inside their symbol. NGC221 would be located below and to the left of the plot; NGC404 and NGC4467 to the left (their  $L_{HX,nuc}$  are upper limits).

the X-ray binaries falling in the extraction region used for the spectrum (Iyomoto et al. 1998).

3) in the realm of low luminosity AGNs, core and power law profiles cover the same range of  $L_{HX,nuc}$  values, and there is no clear trend between  $\gamma$  and  $L_{HX,nuc}$ .

4) the Eddington ratio  $L_{HX,nuc}/L_{Edd}$  is also independent of  $\gamma$  (Fig. 4). Here  $L_{Edd}$  is derived from the  $M_{BH} - \sigma$  relation (e.g., Tremaine et al. 2002), where  $\sigma$  is the central stellar velocity dispersion (from McElroy 1995).  $L_{HX,nuc}/L_{Edd}$  is close to unity only for the Seyfert NGC5548, while it is  $\lesssim 10^{-4}$  for all the other nuclei.

We note that power law galaxies seem to host nuclear emission less frequently than core ones: in Table 2 there are 34 core systems (20 of which are detections) versus 18 power law ones (12 detections). This core/power law proportion is more unbalanced than in Table 1 (where it is 61/47). However, at present we cannot decide whether power law galaxies are less frequently active or they have been chosen less frequently as targets. One reason of preference for pointing core galaxies could be that they are on average brighter; another could be that they include interesting targets as centers of groups/clusters, that in turn generally host activity at a detectable level (see also Sect. 4).

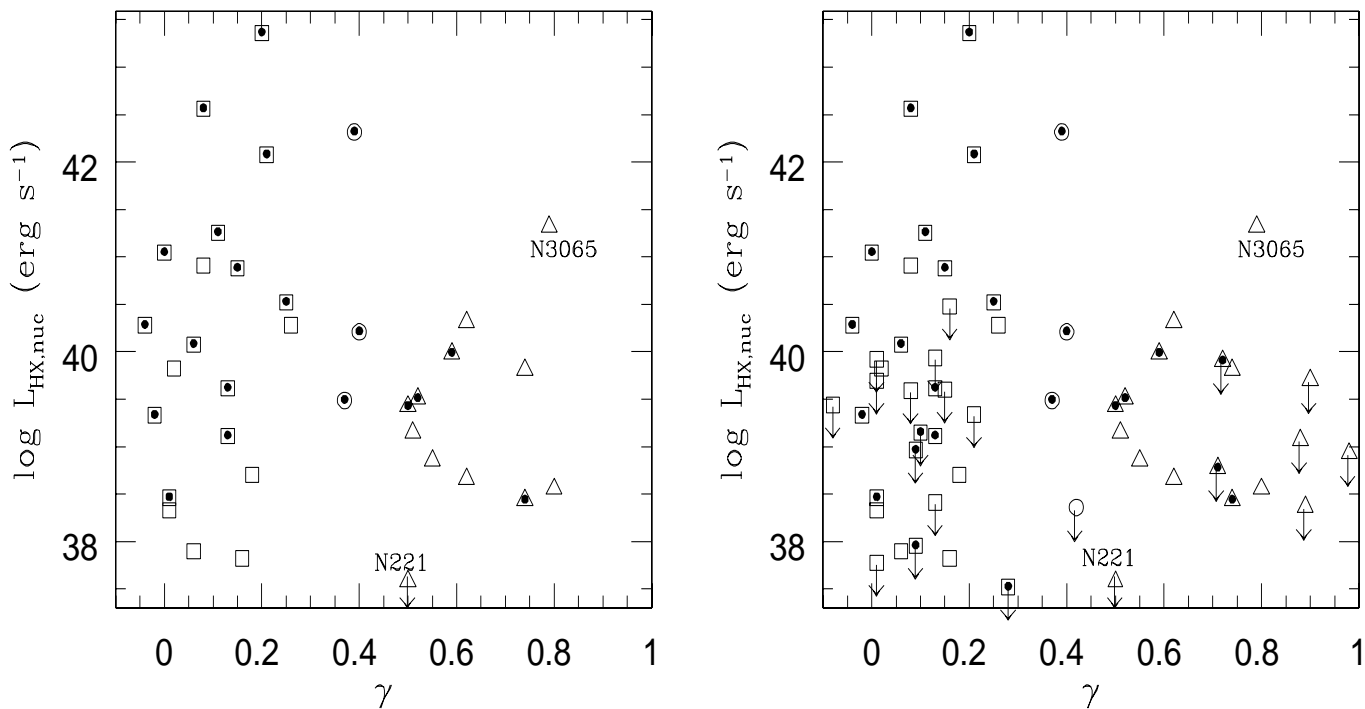


**Figure 3.** The hard nuclear X-ray luminosity  $L_{\text{HX,nuc}}$  versus the shape parameter  $\gamma$  for the galaxies in Table 2 (detections only in the left panel, all data in the right one, with upper limits on  $L_{\text{HX,nuc}}$  shown with a downward arrow). Power law galaxies are shown with triangles, intermediate ones with circles and core ones with squares. Galaxies with an optical nucleus have a dot inside their symbol. The location of NGC221 is below the plot (it is not an upper limit). The four objects with the highest  $L_{\text{HX,nuc}}$  are NGC3862, NGC5548, NGC6166 and NGC7213.

### 3.3 $L_{\text{HX,nuc}}$ and presence of optical nuclei

As mentioned in the Introduction, many galaxies show nuclei, compact light sources that rise above the inward extrapolated surface brightness cusp at small radii. In general these nuclei are bluer than the background starlight and spatially unresolved. They could be nuclear star clusters, in which case they may comprise stars younger or more metal poor than those surrounding the nuclei, or they could be low luminosity AGNs. Ravindranath et al. (2001) argued that the majority of their nuclei are associated with AGNs; Lauer et al. (2005) found nuclei in 29% of core galaxies and 60% of power law ones, with weak evidence that nuclei in power law galaxies have absorption line spectra while those in core galaxies have emission lines. However, since they also found core galaxies with emission lines and no nuclei, the nature of these nuclei remained unknown.

In the sample considered in Table 2 the presence of optical nuclei has been derived from the references giving the slope  $\gamma$ . They are found in  $\sim$ half of the core and  $\sim$  40% of the power law galaxies. As Figs. 2, 3 and 4 show, optical nuclei are present at all  $L_B$  values and, most importantly, at all levels of X-ray activity. Also, there is not a strong relationship between the level of  $L_{\text{HX,nuc}}$  and the frequency of nuclei, except for the fact that all the highest  $L_{\text{HX,nuc}}$  are associated with optical nuclei. It seems reasonable then to conclude that some nuclei are likely associated with nuclear

activity, for the others alternative origins are equally probable.

## 4 DISCUSSION

### 4.1 A dichotomy in hot gas content

The main finding concerning the  $L_{\text{SX,tot}}$  properties of core and power law galaxies is that at any  $L_B$  core systems cover the whole observed range of  $L_{\text{SX,tot}}$  values, while power law systems tend to be underluminous in  $L_{\text{SX,tot}}$  with respect to core ones, especially at high  $L_B$ . If we read  $L_{\text{SX,tot}}$  as a measure of the hot gas content (e.g., Kim et al. 1992), then core galaxies are on average richer of hot gas at any  $L_B$ , and can be very much richer at high  $L_B$ . We discuss here whether these findings are directly linked to the slope of the stellar profile in the inner galactic region or are the result of other different properties of the two families.

Hydrodynamical simulations of the hot gas evolution in early type galaxies give an estimate of their “normal” hot gas content, i.e., that accumulated from stellar mass losses in an isolated galaxy during its lifetime. A set of simulations for spherical galaxy models with central stellar density distributions of the shape found by *HST* was run by Pellegrini & Ciotti (1998). A reason for a different hot gas content of core and power law galaxies was not found, since the *galactic centers* are almost always dense enough to host gas inflows,

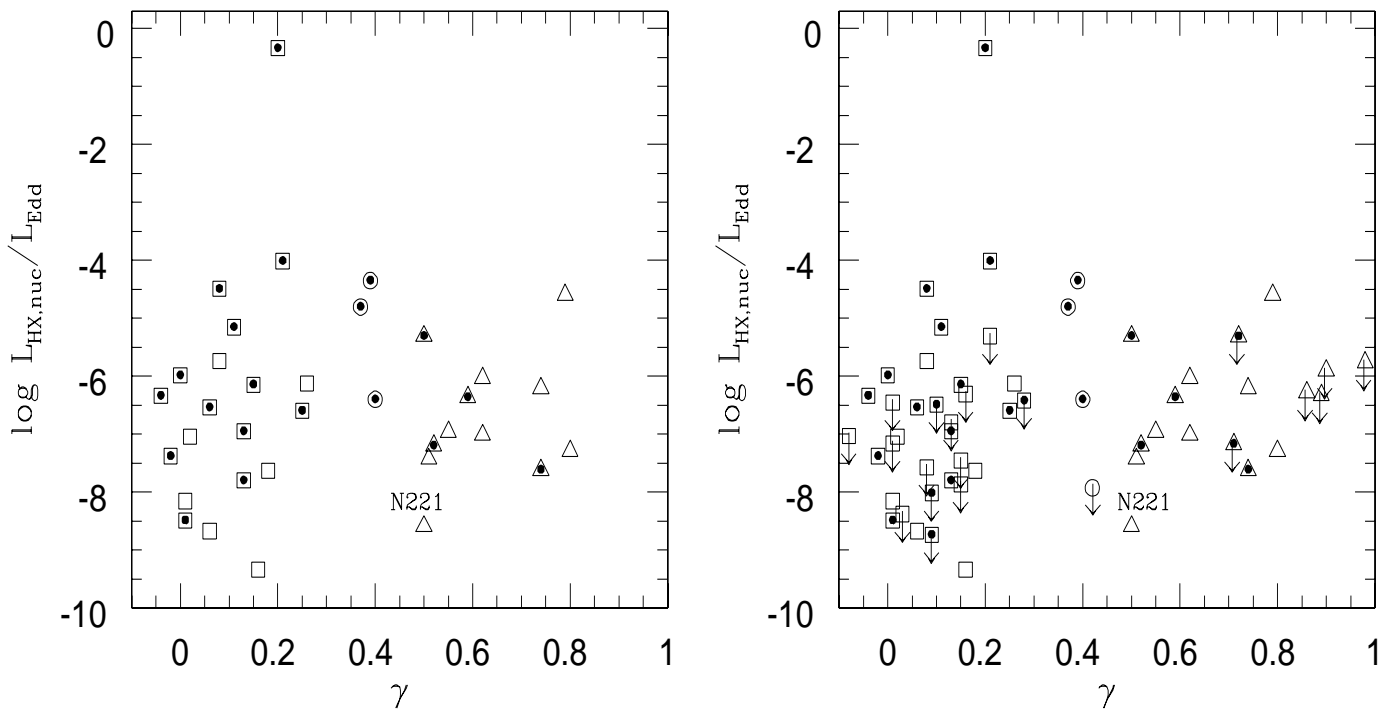


**Figure 4.** The trend of  $L_{\text{HX,nuc}}$  scaled by the Eddington luminosity versus the  $\gamma$  parameter (see Sect. 3.2). Symbols and data are the same as in the previous Fig. 3, with detections only in the left panel, all data in the right one. The only one object with an Eddington ratio close to unity is NGC5548.

regardless of differences in the density profile shapes at the *HST* resolution limit. Instead, another one of the fundamental properties defining the core and power law families likely affects the gas content on the *galactic scale*: power law systems are typically more flattened than core ones of the same  $L_B$  (Sect. 1; Kormendy & Bender 1996, Lauer et al. 2005), and flatter systems are systematically underluminous in X-rays with respect to rounder ones, at fixed  $L_B$  (Eskridge et al. 1995). This was explained by a flatter mass distribution corresponding to a shallower potential well, which makes it easier for the hot gas to escape from the galaxy (Ciotti & Pellegrini 1996, Pellegrini et al. 1997, D’Ercole & Ciotti 1998).

This “global shape” effect can account for the  $\sim 2.6\sigma$  difference in  $L_{\text{SX,tot}}$  shown by the two families at lower  $L_B$  (Sect. 3.1), but it cannot fully explain the very large difference in  $L_{\text{SX,tot}}$  at high  $L_B$ . Actually, the highest  $L_{\text{SX,tot}}$  values of core galaxies cannot be justified within the framework of the above mentioned models. In fact the maximum  $L_{\text{SX,tot}}$  at each  $L_B$  increases with  $L_B$ , since the hot gas is more bound in galaxies that have on average deeper potential wells (e.g., Ciotti et al. 1991), but many core galaxies exceed the maximum values predicted by the models. An additional contribution to their  $L_{\text{SX,tot}}$  may then come from a dense intragroup medium (IGM) or intracluster medium (ICM), not fully subtracted during the data analysis. This subtraction is particularly problematic for galaxies at the center of groups and clusters (O’Sullivan et al. 2001a), and in fact the core galaxies with the highest  $L_{\text{SX,tot}}$  are in

most cases central members of large groups, subclusters or clusters (NGC507, NGC741, NGC1399, NGC3842, IC4329, NGC4073, NGC4486, NGC4889, NGC5419, NGC6166, NGC7619, NGC7768). Instead, no power law systems residing at the center of gas rich groups or clusters are present in the sample considered here. This is in line with the findings for a large sample of central cluster galaxies: their inner light profiles turned out to be typical of core galaxies, with power law profiles only in 10% of them (Laine et al. 2003)<sup>3</sup>. In addition, central dominant galaxies have different X-ray properties compared to non-central members or field galaxies (Helsdon et al. 2001, Matsushita 2001): they show an overluminosity and an extension explained by their hot gas content being more closely correlated with the properties of the group/cluster as a whole than with those of the single galaxy, and also by their being often at the center of a group/cluster cooling flow (e.g., Fabian 1994).

Another significant contribution to  $L_{\text{SX,tot}}$  may come from nuclear activity, as possible for those four core/intermediate objects with the highest  $L_{\text{HX,nuc}}$  of Fig. 3 (see also the next Section). In conclusion, the very large difference in  $L_{\text{SX,tot}}$  at high  $L_B$  is due to properties that belong preferentially to core galaxies, as being central dominant galaxies and/or hosting a bright AGN.

<sup>3</sup> No  $L_{\text{SX,tot}}$  or  $L_{\text{HX,nuc}}$  are available in the literature for these six power law galaxies.

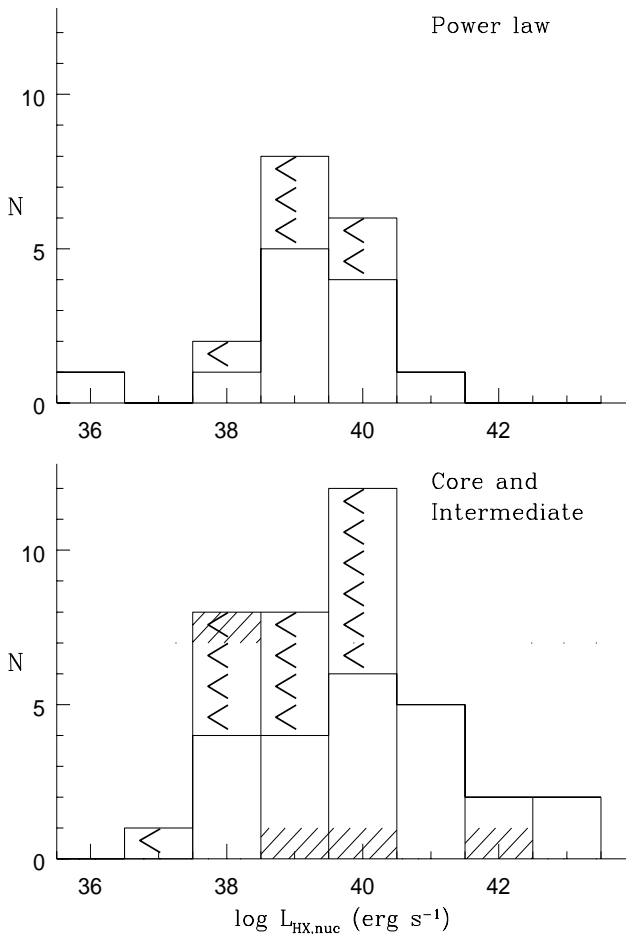


**Figure 5.** The distribution of  $L_{\text{HX,nuc}}$  for power law galaxies (upper panel) and for core plus intermediate galaxies (the latter are four and are indicated with shading; lower panel). Upper limits on  $L_{\text{HX,nuc}}$  are indicated with a “<”.

#### 4.2 A dichotomy in nuclear activity?

The dichotomy found here is that the brightest  $L_{\text{HX,nuc}}$  values, at the level of classical AGNs, are found only for core or intermediate galaxies. This conclusion could actually be hampered by small number statistics; however, a trend of this kind is somewhat expected: nuclear activity is favoured by being the host galaxy the bright central member of a group or cluster (e.g., Burns 1990; here, among the brightest  $L_{\text{HX,nuc}}$  galaxies, NGC6166 resides at the center of Abell 2199 and NGC3862 lies in a dense part of Abell 1367), and the vast majority of central dominant galaxies are core systems (Laine et al. 2003). Actually, it can be concluded that high  $L_{\text{HX,nuc}}$  values are not found in power law galaxies for a sample larger than that in Table 2, as long as nuclear activity is not heavily absorbed and gives a large contribution also to  $L_{\text{SX,tot}}$ , as in Type 1 AGNs (e.g., Antonucci 1993). For example, in NGC3065 most of  $L_{\text{SX,tot}}$  comes from a low luminosity AGN (Sect. 3.1); but this remains the highest  $L_{\text{SX,tot}}$  case of power law galaxies.

Lower activity levels [ $\log L_{\text{HX,nuc}} (\text{erg s}^{-1}) \lesssim 41.3$ ] are instead equally common for all  $\gamma$  values. This is in line with the current belief that all spheroids host a central MBH (Richstone et al. 1998), independently of the shape of their inner light profile. What was not expected a priori is that

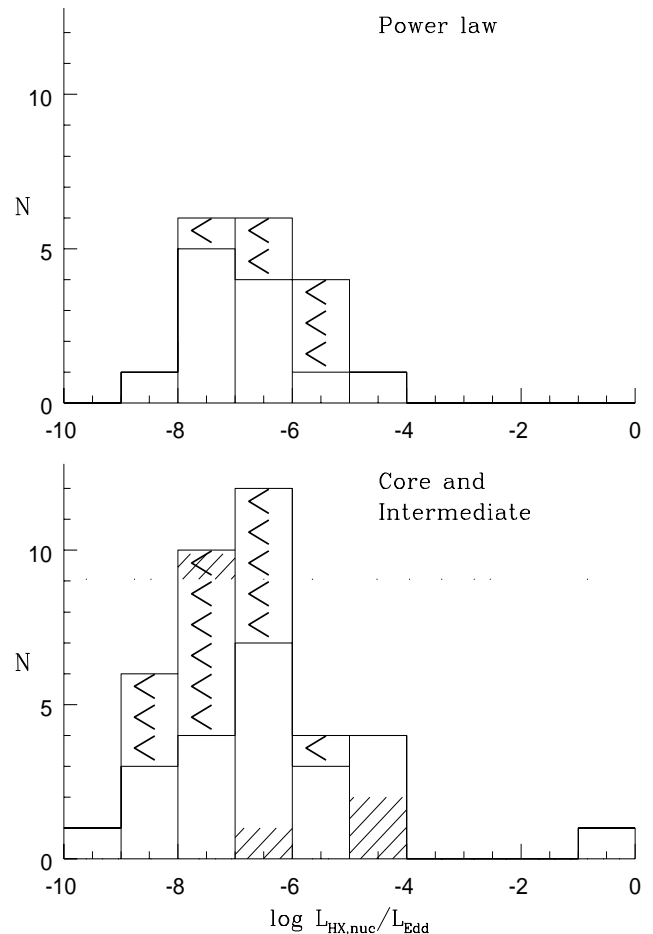


**Figure 6.** The distribution of  $L_{\text{HX,nuc}}/L_{\text{Edd}}$  with symbols as in the previous Fig. 5.

this level of nuclear emission is unrelated with the optical profile shape, that consequently does not play any direct role in the feeding of the central MBH, either in the sense of favouring or opposing it.

Other aspects concerning a possible dichotomy deserve to be explored with a larger sample of power law galaxies. For example, it is to be established whether they really never reach the highest  $L_{\text{HX,nuc}}$  values of core systems, and whether they have a distribution of  $L_{\text{HX,nuc}}$  and  $L_{\text{HX,nuc}}/L_{\text{Edd}}$  significantly different from that of core galaxies (see Figs. 5 and 6). For the data available, a series of Two Sample Tests as those mentioned in Sect. 3.1 shows that the  $L_{\text{HX,nuc}}$  and  $L_{\text{HX,nuc}}/L_{\text{Edd}}$  values of the two families are consistent with being drawn from the same distribution. Another aspect to be investigated is whether power law galaxies are X-ray active less frequently than core ones, as mentioned in Sect. 3.2. Such a tendency is revealed also when nuclear activity is measured by the optical line emission (of the LINER, Seyfert or Transition type; e.g., from Ho et al. 1997). Ravindranath et al. (2001) reported a marginally higher detection frequency of nuclear line emission among core type systems, and optical activity is found in  $\sim$ half of the core galaxies and  $\sim$  1/3 of the power law ones in the Lauer et al. (2005) sample (from their Tab. 3). In the sample considered here (Tables 1 and 2),  $\sim$  60% of core and  $\sim$  1/3 of power law galaxies show optical activity; therefore, in the optical

core systems tend to be active more frequently than power law ones.

### 4.3 Relationship with the galaxy evolution

A few final considerations are presented here to relate the supposed origin and evolution of the two families of core and power law galaxies (described in Sect. 1) with their X-ray properties discussed in this work.

Fig. 3 reminds of the behavior of boxy and disk galaxies with respect to the radio luminosity: boxy galaxies span a large range of radio power values, while disk galaxies are found only at low radio powers (Bender et al. 1989). Given that the radio luminosity and  $L_{\text{HX,nuc}}$  both trace the nuclear activity, this similarity is expected, because boxy galaxies are more frequent among cores systems and power law galaxies among disk ones (Sect. 1). Since the work of Bender et al., the link between boxiness and activity has been explained by boxiness being generally associated with anisotropic (triaxial) systems, where it is easier for the ISM to reach the nucleus than in more rapidly rotating ones. Another suggestion was that boxy and irregular structures are a result of merging processes or various types of interactions (Nieto & Bender 1989), that in turn also seem to trigger nuclear activity (see, e.g., Martini 2004 for a review).

It is unlikely though that the same merging episod created both the fundamental properties of the family of core galaxies (the low rotational level, the boxy isophotes and the ejection of stars from the center with the production of a core) and the onset of the nuclear activity that is still observed today (Fig. 3). In fact the period of activity is  $\lesssim 10^8$  yrs (e.g., Martini 2004), a time that is uncomfortably close to that required for the merging product to reach equilibrium ( $\sim$ few dynamical times, that is  $\sim$ few  $10^8$  yrs in the central galactic regions). Also, nuclear activity of *low level* seems unrelated with the fundamental properties defining the two families of core and power law galaxies (i.e.,  $\gamma$  from Figs. 3 and 4; global isophotal shape from the study on the radio emission by Bender et al. 1989) and likewise is unrelated with the MBH mass and the mass accretion rate on it, estimated under steady state hypotheses (Pellegrini 2005). A comprehensive explanation could be that activity follows cycles of on and off periods, not influenced by long lasting and global properties of the galaxies (Binney & Tabor 1995, Ciotti & Ostriker 2001, Omma et al. 2004, Sazonov et al. 2005). In this context, few systems are expected to show a large  $L_{\text{HX,nuc}}$  value, at the present epoch.

Another aspect concerns the way in which merging affects the galactic hot gas content. In an observational study of the X-ray evolution of on-going mergers, the late stages were found to be underluminous in  $L_{\text{SX,tot}}$  compared with the typical values for early-type galaxies of the same  $L_B$  (Read & Ponman 1998; see also Fabbiano & Schweizer 1995, O’Sullivan et al. 2001b). Although when two galaxies coalesce massive hot extended gas is observed, after this time  $L_{\text{SX,tot}}$  decreases, and the late, relaxed remnants appear devoid of gas. If major mergers are the progenitors of normal ellipticals, the X-ray halo of hot gas must be regenerated. The most plausible mechanism for such a replenishment is through mass losses from evolving stars (Ciotti et al. 1991, O’Sullivan et al. 2001b); this requires many Gyrs to produce the massive ( $\sim 10^9 - 10^{10} M_\odot$ ) hot halos of the core galax-

ies with the highest  $L_{\text{SX,tot}}$  in Fig. 1. Therefore, these must have had their last major merger many Gyrs ago.

## 5 CONCLUSIONS

Core and power law galaxies show a clear dichotomy of properties in the soft X-ray emission, in the sense that core galaxies tend to be more hot gas rich. The main dichotomy in the nuclear hard X-ray emission is the lack of bright nuclei among power law galaxies (to be tested with a larger sample of the latter). More in detail, the results of this work can be summarized as follows:

1. At any  $L_B$  core galaxies cover the whole range of observed  $L_{\text{SX,tot}}$  values; this can be very large ( $\sim 2$  orders of magnitude) at  $\log L_B (L_\odot) > 10.4$ , reaching  $L_{\text{SX,tot}} \gtrsim 10^{42}$  erg s $^{-1}$ . Power law galaxies tend to be underluminous in  $L_{\text{SX,tot}}$  with respect to core ones at every  $L_B$ , and especially at high  $L_B$ .
2. The above properties are not directly resulting from the shape of the inner optical profile. The underluminosity of power law galaxies has a contribution from their average flatter mass distribution, which favors the gas outflow. The large overluminosity in  $L_{\text{SX,tot}}$  of core systems of high  $L_B$  is often linked to their being central dominant galaxies. Instead, power law systems at the center of hot gas rich groups or clusters are lacking from this sample (as are not found in such a position in general).
3. The highest nuclear luminosities in the 2–10 keV band are reached by core or intermediate galaxies. In the low luminosity AGN domain,  $L_{\text{HX,nuc}}$  is independent of  $\gamma$ : core and power law profiles correspond to the same large range of  $L_{\text{HX,nuc}}$ , with no trend with  $\gamma$ . The Eddington ratio  $L_{\text{HX,nuc}}/L_{\text{Edd}}$  is always very low ( $\lesssim 10^{-4}$ ), except for one core galaxy, again without any trend with  $\gamma$ .
4. Intermediate galaxies share the same  $L_{\text{SX,tot}}$  and  $L_{\text{HX,nuc}}$  properties as core ones.
5. The presence of nuclear hard emission seems more frequent among core galaxies than power law ones, as seems also to be the case for optical line emission.
6. The presence of optical nuclei is unrelated with the level of nuclear hard emission. The highest  $L_{\text{HX,nuc}}$ , though, are all associated with optical nuclei.
7. It is unlikely that the same merging episod was responsible for the building of the galactic structure (e.g., the isophotal shape, the  $\gamma$  value) and the nuclear activity observed today. The latter appears mostly of low level and unrelated with the global galaxy properties (including  $\gamma$ ). Also the hot massive haloes of many core galaxies suggest that their last major merging episod took place many Gyrs ago.

## ACKNOWLEDGMENTS

I warmly thank Ji-Feng Liu for providing the upper limits on the flux for 7 of the objects listed in Table 2 and the referee for useful comments. I acknowledge use of the NASA Extragalactic database (NED), operated by the Jet Propulsion Laboratory, California Institute of Technology, and of the LEDA database.



**Table 1.** Properties of galaxies with  $\gamma$  and  $L_{\text{SX,tot}}$  measured

Name	$d^a$ (Mpc)	$\log L_B^b$ ( $L_{B\odot}$ )	$\log L_{\text{SX,tot}}^c$ ( $\text{erg s}^{-1}$ )	$\gamma^d$	Ref.
Core:					
NGC404	2.4	8.47	<38.28	0.28	Ra
NGC507	60.3	10.87	42.61	0.00	L
NGC524	24.0	10.43	<39.87	0.03	Ra
NGC584	20.1	10.28	<40.01	0.30	L
NGC720	27.7	10.63	40.86	0.06	F
NGC741	67.1	10.98	41.81	0.10	L
NGC1016	71.8	10.93	41.26	0.09	L
NGC1052	19.4	10.20	40.39	0.11	Ra
NGC1316	21.5	11.08	41.02	0.13	L
NGC1374	19.8	10.06	39.97	-0.03	L
NGC1399	20.0	10.60	41.71	0.09	L
NGC1400	26.4	10.36	40.34	0.00	F
NGC1600	60.8	11.04	41.55	0.08	F
NGC1700	38.4	10.61	40.68	0.07	L
NGC2300	28.8	10.44	41.19	0.08	L
NGC2832	87.1	11.07	41.63	0.02	F
NGC2841	13.0	10.62	39.98	0.01	F
NGC2986	30.7	10.52	40.97	0.18	Re
NGC3193	34.0	10.55	40.36	0.01	Re
NGC3379	10.6	10.11	<39.59	0.18	L
NGC3607	22.8	10.58	40.66	0.26	L
NGC3608	22.9	10.24	40.14	0.17	L
NGC3613	29.1	10.42	<40.18	0.04	Re
NGC3640	27.0	10.57	40.06	0.03	L
NGC3706	44.4	10.53	<41.34	-0.01	L
NGC3842	91.8	11.02	41.90	0.15	L
NGC4073	87.2	11.15	42.46	-0.08	L
NGC4168	34.1	10.41	40.57	0.17	Re
NGC4261	31.6	10.70	41.21	0.00	Ra
NGC4278	16.1	10.23	40.35	0.10	L
NGC4291	26.1	10.05	40.94	0.02	L
NGC4365	20.4	10.56	40.47	0.09	L
NGC4374	18.4	10.70	40.96	0.13	Ra
NGC4382	18.4	10.77	40.46	0.01	L
NGC4406	17.1	10.73	42.12	-0.04	L
NGC4458	17.2	9.57	39.90	0.17	L
NGC4472	16.3	10.92	41.45	0.01	L
NGC4473	15.7	10.13	40.12	0.01	L
NGC4476	17.2	9.50	<40.34	0.21	Fe
NGC4478	18.1	9.90	<40.52	0.10	L
NGC4486	16.1	10.86	42.96	0.25	F
NGC4552	15.4	10.26	40.68	-0.02	L
NGC4589	22.0	10.23	40.26	0.25	L
NGC4636	14.7	10.44	41.52	0.13	Ra
NGC4649	16.8	10.78	41.33	0.16	L
NGC4709	35.3	10.49	40.55	0.28	L
NGC4874	89.5	11.07	41.83	0.13	F
NGC4889	89.5	11.20	42.77	0.05	F
NGC5061	25.4	10.56	39.96	0.05	L
NGC5077	30.6	10.27	40.49	0.23	Re
NGC5198	35.5	10.29	<40.39	0.23	Re
NGC5419	59.2	10.97	41.89	0.03	L
NGC5576	25.6	10.30	<40.28	0.26	L
NGC5903	33.9	10.58	<40.63	0.13	Re
NGC5982	38.3	10.55	41.18	0.05	L
NGC6166	110.1	11.21	43.94	0.08	F
NGC6876	54.4	10.93	41.61	0.00	L
NGC7619	53.0	10.82	41.87	0.01	L
NGC7768	93.2	10.93	41.75	0.00	F
IC1459	29.2	10.75	41.09	0.15	L

**Table 1 – continued**

Name	$d^a$ (Mpc)	$\log L_B^b$ ( $L_{B\odot}$ )	$\log L_{\text{SX,tot}}^c$ ( $\text{erg s}^{-1}$ )	$\gamma^d$	Ref.
IC4329	53.6	10.78	41.89	0.01	L
Intermediate:					
NGC821	24.1	10.28	<40.45	0.42	L
NGC3585	20.0	10.58	39.98	0.31	L
NGC3862	83.1	10.57	41.91	0.39	C
NGC4594	9.8	10.74	40.42	0.40	C
NGC5273	16.5	9.65	39.83	0.37	Ra
NGC5831	27.2	10.18	<40.40	0.33	Re
NGC5898	29.1	10.39	<40.48	0.41	Re
NGC7626	53.0	10.85	41.30	0.36	Ra
Power law:					
NGC221 (M32)	0.81	8.46	37.87	0.50	Ra
NGC596	21.7	10.19	<39.58	0.54	L
NGC1172	21.5	9.85	<40.34	1.01	F
NGC1351	21.0	9.91	<40.46	0.78	Q
NGC1426	24.1	10.06	<40.15	0.56	L
NGC1427	23.6	10.23	40.08	0.51	L
NGC1439	26.6	10.22	<40.22	0.74	L
NGC1553	18.5	10.84	40.73	0.74	Q
NGC2434	21.6	10.26	40.27	0.75	L
NGC2634	33.4	10.07	<40.46	0.81	Re
NGC2685	16.1	9.81	<40.11	0.73	Ra
NGC2778	22.9	9.59	<40.12	0.83	L
NGC2974	21.5	10.26	40.34	0.62	L
NGC3065	30.4	9.75	41.02	0.79	Re
NGC3078	35.2	10.52	40.76	0.95	Re
NGC3115	9.7	10.18	39.80	0.52	L
NGC3377	11.2	9.82	<39.70	0.62	L
NGC3384	11.6	9.98	<39.65	0.71	L
NGC3599	20.3	9.68	<39.25	0.79	F
NGC3605	20.7	9.51	39.12	0.67	F
NGC3610	21.4	10.19	39.62	0.76	L
NGC4239	17.0	9.25	<39.86	0.65	F
NGC4342	16.1	9.31	<40.16	1.47	Fe
NGC4387	21.4	9.73	39.97	0.72	F
NGC4417	16.1	9.78	<40.69	0.71	Ra
NGC4434	26.7	9.90	<40.28	0.70	F
NGC4464	16.1	9.21	<39.82	0.88	F
NGC4467	16.1	8.70	<39.30	0.98	F
NGC4474	16.1	9.65	<39.86	0.72	Re
NGC4494	17.0	10.67	39.91	0.55	L
NGC4503	16.1	9.78	<39.89	0.64	Re
NGC4550	15.8	9.72	39.78	0.89	Fe
NGC4551	17.3	9.65	<39.16	0.80	F
NGC4564	15.0	9.81	<39.80	0.80	Re
NGC4621	18.3	10.44	40.14	0.85	L
NGC4648	24.8	9.88	<39.90	0.92	Re
NGC4660	16.1	9.75	<39.40	0.91	L
NGC4697	11.7	10.33	39.90	0.74	F
NGC4742	15.5	9.75	<39.99	1.09	F
NGC4881	89.5	10.34	<40.33	0.76	F
NGC5308	28.2	10.21	<40.02	0.82	Re
NGC5812	26.9	10.27	<40.40	0.59	Re
NGC5838	23.2	10.21	40.03	0.93	Ra
NGC5845	26.0	9.67	<40.05	0.51	F
NGC7332	23.0	10.21	<40.36	0.90	F
NGC7457	13.2	9.96	<39.68	0.61	L
NGC7743	20.7	9.93	39.58	0.50	Ra

<sup>a</sup> Distance (see Sect. 2).

<sup>b</sup> Blue band luminosity (see Sect. 2).

<sup>c</sup> Soft X-ray luminosity for the whole galaxy (see Sect. 2).

**Table 1** – *continued*

<sup>d</sup> Slope of the surface brightness profile in the central region ( $I \propto R^{-\gamma}$ ). The references for the  $\gamma$  values are given in the last column: (L) Lauer et al. 2005; (Re) Rest et al. 2001; (F) Faber et al. 1997; (Ra) Ravindranath et al. 2001; (Fe) Ferrarese et al. 1994; (Q) Quillen et al. 2000; (C) Crane et al. 1993.

**REFERENCES**

- Antonucci, R. 1993, ARA&A 31, 473  
 Bender R., Surma P., Döbereiner S., Möllenhoff C., Madejsky R. 1989, A&A 217, 35  
 Bianchi, S., Matt, G., Balestra, I., Guainazzi, M., Perola, G. C. 2004, A&A 422, 65  
 Biller, B.A., Jones, C., Forman, W.R., Kraft, R., & Ensslin, T. 2004, ApJ, 613, 238  
 Binney J., Tabor G. 1995, MNRAS 276, 663  
 Blanton, E.L., Sarazin, C.L., & Irwin, J.A. 2001, ApJ, 552, 106  
 Burns, J.O. 1990, AJ, 99, 14  
 Ciotti L., D’Ercole A., Pellegrini S., Renzini A. 1991, ApJ 376, 380  
 Ciotti L., Pellegrini S. 1996, MNRAS 279, 240  
 Ciotti, L., & Ostriker, J.P. 2001, ApJ, 551, 131  
 Cipollina M., Bertin G. 1994, A&A 288, 43  
 Colbert, E.J.M., Mushotzky, R.F. 1999, ApJ, 519, 89  
 Crane P., et al. 1993, AJ 106, 1371  
 David, L.P., Jones, C., Forman, W., Murray, S. 2005, submitted to ApJ(astro-ph/0506018)  
 D’Ercole, A., Ciotti, L. 1998, ApJ494, 535  
 Donato, D., Sambruna, R. M., Gliozzi, M. 2004, ApJ617, 915  
 Dow K.L., White S.D.M. 1995, ApJ 439, 113  
 Dudik, R. P., Satyapal, S., Gliozzi, M., Sambruna, R. M. 2005, ApJ620, 113  
 Eracleous, M., Halpern, J.P. 2001, ApJ 554, 240  
 Eskridge, P.B., Fabbiano, G., Kim, D.W. 1995, ApJ442, 523  
 Fabbiano G., Kim D.W., Trinchieri G. 1992, ApJS 80, 531  
 Fabbiano, G., Schweizer, F. 1995, ApJ447, 572  
 Fabbiano, G., Juda, J.Z. 1997, ApJ476, 666  
 Fabbiano, G., Elvis, M., Markoff, S., Siemiginowska, A., Pellegrini, S., Zezas, A., Nicastro, F., Trinchieri, G., & McDowell, J. 2003, ApJ, 588, 175  
 Fabbiano, G., Baldi, A., Pellegrini, S., Siemiginowska, A., Elvis, M., Zezas, A., & McDowell, J. 2004, ApJ, 616, 730  
 Faber, S.M., Tremaine, S., Ajhar, E.A., et al. 1997, AJ 114, 1771  
 Fabian, A. C. 1994, ARA&A 32, 277  
 Feigelson, E.D., Nelson, P.I. 1985, ApJ293, 192  
 Ferrarese L., van den Bosch F.C., Ford H., Jaffe W., O’Connell R. 1994, AJ 108, 1598  
 Filho, M. E., Fraternali, F., Markoff, S., Nagar, N. M., Barthel, P. D., Ho, L. C., & Yuan, F. 2004, A&A, 418, 429  
 Graham, Alister W.; Erwin, Peter; Caon, N.; Trujillo, I. 2001, ApJ 563, L11  
 Helsdon, S.F., Ponman, T.J., O’Sullivan, E., Forbes, D.A. 2001, MNRAS 325, 693  
 Ho, L.C., Filippenko, A. V., & Sargent, W.L. W. 1997, ApJ, 487, 568  
 Ho, L. C., Terashima, Y., & Ulvestad, J.S. 2003, ApJ, 589,

**Table 2.** Properties of galaxies with  $\gamma$  and  $L_{\text{HX,nuc}}$  measured

Name	d <sup>a</sup> (Mpc)	log L <sub>B</sub> <sup>b</sup> (L <sub>B⊙</sub> )	log L <sub>HX,nuc</sub> <sup>c</sup> (erg s <sup>-1</sup> )	$\gamma^d$		
Core:						
NGC404	2.4	8.47	<37.52	Liu	0.28	Ra
NGC507	60.3	10.87	<39.92	Do	0.01	L
NGC720	27.7	10.63	37.90	Je	0.06	F
NGC1052	19.4	10.20	41.26	Du	0.11	Ra
NGC1316	21.5	11.08	39.62	KF	0.13	L
NGC1399	20.0	10.60	<38.96	Lo	0.09	L
NGC1600	60.8	11.04	<39.59	Si	0.08	F
NGC2300	28.8	10.44	40.91	LB	0.08	L
NGC2841	13.0	10.62	38.33	Du	0.01	F
NGC3193	34.0	10.55	<39.69	RW	0.01	Re
NGC3379	10.6	10.11	38.70	Da	0.18	L
NGC3607	22.8	10.58	40.28	Te	0.26	L
NGC3842	91.8	11.02	<39.6	Su	0.15	L
NGC4261	31.6	10.70	41.05	Do	0.00	Ra
NGC4278	16.1	10.23	40.08	Du	0.06	L
NGC4291	26.1	10.05	39.82	RW	0.02	L
NGC4365	20.4	10.56	<37.96	Si03	0.09	L
NGC4374	18.4	10.70	39.11	Du	0.13	Ra
NGC4382	18.4	10.77	<37.78	Si03	0.01	L
NGC4406	17.1	10.73	40.28	CM	-0.04	L
NGC4472	16.3	10.92	38.46	Bil	0.01	L
NGC4476	17.2	9.50	<39.34	Liu	0.21	Fe
NGC4478	18.1	9.90	<39.15	Liu	0.10	L
NGC4486	16.1	10.86	40.52	Du	0.25	F
NGC4552	15.4	10.26	39.33	Fi	-0.02	L
NGC4636	14.7	10.44	<38.41	Lo	0.13	Ra
NGC4649	16.8	10.78	37.82	Sol	0.16	L
NGC4874	89.5	11.07	<39.94	Do	0.13	F
NGC5548	68.9	10.67	43.36	Bi	0.20	Ra
NGC5813	32.2	10.68	<39.44	Liu	-0.08	L
NGC6166	110.1	11.21	42.56	Do	0.08	F
NGC7052	62.4	10.50	<40.48	Do	0.16	Q
NGC7213	21.5	10.22	42.08	Bi	0.21	L
IC1459	29.2	10.75	40.88	Fa	0.15	L
Intermediate:						
NGC821	24.1	10.28	<38.36	Fa04	0.42	L
NGC3862	83.1	10.57	42.32	Do	0.39	C
NGC4594	9.8	10.74	40.21	Pe	0.40	C
NGC5273	16.5	9.65	39.49	LB	0.37	Ra
Power law:						
NGC221	0.81	8.46	35.97	Ho	0.50	Ra
NGC1553	18.5	10.84	39.81	Bl	0.74	Q
NGC2974	21.5	10.26	40.32	LB	0.62	L
NGC3065	30.4	9.75	41.32	Iy	0.79	Re
NGC3115	9.7	10.18	39.5	LB	0.52	L
NGC3377	11.2	9.82	38.66	RW	0.62	L
NGC3384	11.6	9.98	<38.77	RW	0.71	L
NGC4143	15.9	9.91	39.98	TW	0.59	Ra
NGC4387	21.4	9.73	<39.90	CM	0.72	F
NGC4464	16.1	9.21	<39.07	Liu	0.88	F
NGC4467	16.1	8.70	<38.93	Liu	0.98	F
NGC4494	17.0	10.67	38.86	Du	0.55	L
NGC4550	15.8	9.72	<38.36	TW	0.89	Fe
NGC4564	15.0	9.81	38.56	So	0.80	Re
NGC4697	11.7	10.33	38.44	Sa	0.74	F
NGC5845	26.0	9.67	39.15	So	0.51	F
NGC7332	23.0	10.21	<39.70	Liu	0.90	F
NGC7743	20.7	9.93	39.43	Te	0.50	Ra

<sup>a</sup> Distance, as for Tab. 1.

**Table 2** – *continued*

<sup>b</sup> Blue band luminosity for the whole galaxy, as for Tab. 1.

<sup>c</sup> Nuclear X-ray luminosity in the 2–10 keV band. References for the X-ray luminosity values are given in the next column: (Bi) Bianchi et al. (2004); (Bil) Biller et al. 2004; (Bl) Blanton et al. 2001; (CM) Colbert & Mushotzky (1999); (Da) David et al. (2005); (Do) Donato et al. 2004; (Du) Dudik et al. 2005; (Fa) Fabbiano et al. 2003; (Fa04) Fabbiano et al. 2004; (Fi) Filho et al. 2004; (Ho) Ho et al. 2003; (Iy) Iyomoto et al. 1998; (Je) Jeltema et al. 2003; (KF) Kim & Fabbiano 2003; (LB) Liu & Bregman (2005); (Liu) Ji-Feng Liu (private comm., based on LB); (Lo) Loewenstein et al. 2001; (Pe) Pellegrini et al. 2003; (RW) Roberts & Warwick 2000; (Sa) Sarazin et al. 2001; (Si) Sivakoff et al. 2004; (Si03) Sivakoff et al. 2003; (So) Soria et al. 2005, submitted to ApJ; (Sol) Soldatenkov et al. 2003; (Su) Sun et al. (2005); (Te) Terashima, Ho & Ptak 2000; (TW) Terashima & Wilson 2004.

<sup>d</sup> Slope of the central profile, and references for the  $\gamma$  values in the next column, as for Tab. 1.

783

Irwin J.A., Sarazin C.L. 1998, ApJ 499, 650  
 Iyomoto, N., Makishima, K., Matsushita, K., Fukazawa, Y., Tashiro, M., Ohashi, T. 1998, ApJ 503, 168  
 Jeltema, T.E., Canizares, C.R., Buote, D.A., & Garmire, G.P. 2003, ApJ, 585, 756  
 Kim D.W., Fabbiano G., Trinchieri G. 1992, ApJ 393, 134  
 Kim, D. W., & Fabbiano, G. 2003, ApJ, 586, 826  
 Kormendy J., Bender R. 1996, ApJ 464, L119  
 Laine, S., van der Marel, R.P., Lauer, T.R., Postman, M., O’Dea, C.P., Owen, F.N. 2003, AJ 125, 478  
 Lauer T.R., et al. 1995, AJ 110, 2622  
 Lauer T.R., et al. 2005, AJ 129, 2138  
 Liu, Ji-F., Bregman, J.N. 2005, ApJS 157, 59  
 Lowenstein, M., Mushotzky, R.F., Angelini, L., Arnaud, K.A., & Quataert, E. 2001, ApJ, 555, L21  
 Martini, P. 2004, in "Coevolution of Black Holes and Galaxies", Cambridge University Press, Carnegie Observatories Astrophysics Series. Ed. L. C. Ho, p. 170.  
 Matsushita, K. 2001, ApJ, 547, 693  
 Milosavljevic, M., Merritt, D., Rest, A., van den Bosch, F.C. 2002, MNRAS331, L51  
 Naab, T., Burkert, A. 2003, ApJ 597, 893  
 O’Sullivan, E., Forbes, D.A., Ponman, T.J. 2001a, MNRAS 328, 461  
 O’Sullivan, E., Forbes, D.A., Ponman, T.J. 2001b, MNRAS 324, 420  
 O’Sullivan, E., Ponman, T.J. 2004, MNRAS 349, 535  
 Omma, H., Binney, J., Bryan, G., & Slyz, A. 2004, MNRAS, 348, 1105  
 Nieto, J.-L., Bender, R. 1989, A&A, 215, 266  
 Pellegrini S., Held E., Ciotti L. 1997, MNRAS, 288, 1  
 Pellegrini S., Ciotti L. 1998, A&A 333, 433  
 Pellegrini, S. 1999, A&A 351, 487  
 Pellegrini, S., Baldi, A., Fabbiano, G., & Kim, D.W. 2003, ApJ, 597, 175  
 Pellegrini, S. 2005, ApJ, 624, 155  
 Quillen A.C., Bower G.A., Stritzinger M. 1999, submitted to ApJ  
 Ravindranath, S., Ho, L.C., Peng, C.Y., Filippenko, A.V., Sargent, W.L.W. 2001, AJ 122, 653  
 Read, A. M., Ponman, T. J. 1998, MNRAS 297, 143  
 Rest, A., van den Bosch, F.C., Jaffe, W., Tran, H., Tsve-

tanov, Z., Ford, H. C., Davies, J., Schafer, J. 2001, AJ 121, 243  
 Richstone D., et al. 1998, Nature 395, A14  
 Roberts, T. P., Warwick, R. S. 2000, MNRAS315, 98  
 Sarazin, C. L., Irwin, J.A., & Bregman, J.N. 2001, ApJ, 556, 533  
 Sazonov, S.Yu., Ostriker, J.P., Ciotti, L., Sunyaev, R.A. 2005, MNRAS, 358, 168  
 Sivakoff, G.R., Sarazin, C.L., & Irwin, J.A. 2003, ApJ, 599, 218  
 Sivakoff, G.R., Sarazin, C.L., & Carlin, J.L. 2004, ApJ, 617, 262  
 Soldatenkov, D. A., Vikhlinin, A. A., & Pavlinsky, M. N. 2003, AstL, 29, 298  
 Sun, M., Vikhlinin, A., Forman, W., Jones, C., Murray, S.S. 2005, ApJ619, 169  
 Terashima, Y., Ho, L.C., Ptak, A. 2000, ApJ539, 161  
 Terashima, Y., Iyomoto, N., Ho, L.C., Ptak, A. 2002, ApJS 139, 1  
 Terashima, Y., & Wilson, A. S. 2004, ApJ583, 145  
 Tonry, J.L., Dressler, A., Blakeslee, J.P., et al. 2001, ApJ, 546, 681  
 Tremaine, S., Gebhardt, K., Bender, R., et al. 2002, ApJ574, 740  
 Trujillo, I., Erwin, P., Asensio Ramos, A., Graham, A.W. 2004, AJ 127, 1917  
 van der Marel R.P. 1999, ApJ 117, 744